Journal of Earth Science, *Vol. 22*, *No. 6*, *p. 688–703*, *December 2011* *ISSN 1674-487X*
Printed in China
DOI: 10.1007/s12583-011-0220-7

Geochemistry of Middle Triassic Radiolarian Cherts from Northern Thailand: Implication for Depositional Environment

Hathaithip Thassanapak
Department of Biology, *Faculty of Science*, *Mahasarakham University*, *Mahasarakham* 44150, *Thailand*
Mongkol Udchachon*
Palaeontological Research and Education Centre, *Mahasarakham University*, *Mahasarakham* 44150, *Thailand*
Chongpan Chonglakmani
School of Geotechnology, *Institute of Engineering*, *Suranaree University of Technology*, *Nakhon Ratchasima* 30000, *Thailand*
Qinglai Feng (冯庆来)
State Key Laboratory of Geological Processes and Mineral Resources, *China University of Geosciences*, *Wuhan* 430074, *China*

ABSTRACT: Geochemical analysis reveals that Middle Triassic radiolarian cherts from northern Thailand, including Chiang Dao, Lamphun and Den Chai, are of biogenic origin. These cherts present slightly high SiO_2 content which was possibly modified by diagenetic alteration and migration processes as indicated by negative correlation between SiO_2 and most of the other major elements. The relatively high content of Cr, Zr, Hf, Rb and Th and high positive correlation of these elements with Al and Ti from the majority of cherts suggest a close relation to terrigenous component. The Ce anomaly (Ce/Ce*) with geometric means ranging from 0.85 to 0.93 is compatible with that of continental margin composition (0.67–1.52) from Murray et al. (1990) which is also consistent with low Eu anomalies (Eu/Eu*, 0.91–0.94). Moreover, the slightly low ratios of La and Ce NASC normalized (La_n/Ce_n, 0.91–0.94) and the low LREE and HREE ratios in most of our samples (La_n/Yb_n, 0.62–0.85) are in agreement with the continental margin. The result from La_n/Ce_n vs. $Al_2O_3/(Al_2O_3+Fe_2O_3)$ discrimination diagrams also supports the continental margin (residual basin, *s. str.*) interpretation. These geochemical results are compatible with geological evidence, which suggest that during the Middle Triassic, radiolarian cherts were deposited within a deeper part of a residual basin in which an accommodation space was possibly controlled by faults under extensional regime subsequent to Late Variscan (Permian) orogeny. Paleogeographically, the main Paleotethys which closed during Late Triassic should be located further to the west of these study localities. This scenario is in

This study was supported mainly by the National Natural Science Foundation of China (No. 40772143), the Special Fund of the State Key Laboratory of Geological Processes and Mineral Resources, China University of Geosciences, and the Faculty of Science, Mahasarakham University.
*Corresponding author: mongkol.c@msu.ac.th

Manuscript received May 28, 2010.
Manuscript accepted September 17, 2010.

agreement with the current view of the Tethys in this part of the world.

KEY WORDS: Triassic, geochemistry, radiolarian chert, depositional environment, northern Thailand.

INTRODUCTION

The occurrences of Middle Triassic radiolarian cherts in northern Thailand have been reported for the last few decades by several radiolarian workers (e.g., Thassanapak et al., 2011, 2007; Feng et al., 2005b, 2002; Kamata et al., 2002; Caridroit, 1993; Sashida et al., 1993). These studies provide critical information not only about the stratigraphic position of the sequences but also to the geodynamic scenario. In this region, the study of Triassic radiolarian cherts is important since it is related to the final evolution of the main Paleotethys. Recently, it has been widely accepted that the main Paleotethys is situated along the Thai-Myanmar border (Ferrari et al., 2008; Ueno, 2003; Chonglakmani, 2002, 1999; Wang et al., 2001). However, due to the lack of index fossils in some parts of this region, geological mapping is difficult. The ages of some rock sequences were interpreted largely by means of lithologic characters and stratigraphic superposition. Current studies on Triassic radiolarian cherts, which mostly present a close relation to clastic sequences, are important for age revision. Geochemical composition of cherts in this region, however, is still poorly known. In order to have a better understanding of the depositional environment of the Middle Triassic radiolarian cherts, geochemical analysis of major, trace and rare earth elements was carried out. Selected sections of Middle Triassic radiolarian cherts and siliceous rocks from the central part of northern Thailand were investigated. The results from this study could enable a comparison of the geochemical compositions of siliceous rocks and their paleogeographic position between this study area and others areas in the eastern part of Paleotethys.

GEOLOGICAL SETTING

The Triassic sedimentary sequences in Thailand consist of four main facies, including the continental, continental platform, marine associated with volcanic, and deep marine facies (Chonglakmani, 2002). The continental facies is extensively exposed in the Indochina block which is located to the east of Nan-Uttaradit suture and the rest are observed in the Shan-Thai block which is situated to the west of the suture. All of our study sections are from Middle Triassic chert and siliceous rock sequences, observed in the Shan-Thai block in the vicinity of Chiang Dao, Lamphun and Den Chai (Fig. 1). The Chiang Dao area is located to the north of Chiang Mai, northern Thailand. This area is occupied mainly by Carboniferous clastic sequences. Middle Triassic granite and granodiorite were unearthed mainly in the west and the south of the area. Permian limestones were exposed to the south and the north of this area (Hess and Koch, 1979). Deep sea deposits were reported in the north of Chiang Dao, known as "Fang Chert", which range from Devonian to Middle Triassic (Caridroit, 1993; Sashida et al., 1993; Jaeger et al., 1969). Lamphun is located close to the southern portion of the Cenozoic Chiang Mai basin. This area consists mainly of Carboniferous and Permian strata exposed to the west of the Mae Tha fault. The Carboniferous strata consist of greywackes, arkosic protoquartzites and orthoquartzites, quartzites and shales. The Lower Permian is composed of phyllites, sandstones, schists, siltstones, quartzites, quartzitic schists, agglomerates and tuffs. The Middle Permian consists of massive limestones, calcareous shales and sandstones. There are outcrops of Silurian–Devonian metamorphic rocks and Triassic granite to the east of the fault. Quaternary sediment is deposited in the basin and in the valley along the fault (Charoenprawat et al., 1994). Den Chai is located at the southern edge of the Cenozoic Phrae basin. This area is covered mainly by Triassic rocks and Pleistocene basalts (Geological Survey Division, 1999). The Triassic rocks consist of the Pha Daeng Formation of the Lampang Group. The rocks are characterized mainly by sandstones, siltstone and shales with Bouma sequences which were interpreted as shallow marine and fan-delta facies deposited on the extensional forearc basin (Chaodumrong and Burret, 1997). However, these flysch-like strata could be a consequence of sediment deposited on a rapidly subsiding area of epicontinental setting (intramontane basins)

(Helmcke, 1994). Bivalves including *Halobia* sp., *Palaeocardita* sp., and *Posidonia* sp. indicate a Late Triassic date for the formation (Meesook et al., 2002; Chonglakmani and Grant-Mackie, 1993).

DESCRIPTION OF STUDY SECTIONS

The Chiang Dao Section is located in the area of Ban Nawai north of Chiang Dao District, Chiang Mai Province. This road-cut section is characterized by a folded chert sequence exposed on the western part of Highway 1322 at 1.5 km. This sequence is approximately 9 m thick, underlain by sandstone and overlain by mudstone strata (Fig. 1). The bedded cherts are mostly light brown and grey in color with a bed thickness of 3–10 cm, and commonly observed with claystone parting and siliceous shale intercalation. The age of the section determined from radiolarians is restricted to Middle Triassic (Thassanapak et al., 2011). The Lamphun Section is exposed by a road cut and is located to the east of Highway 11 at 59.2 km within the area of Ban Cham Bon Village, Muang District, Lamphun Province. The outcrop is characterized by a folded chert sequence embedded in a light-brown mudstone sequence, of which is difficult to estimate the total thickness. The cherts are brown and light grey with bed thicknesses ranging between 5 and 10 cm and commonly found with a shale parting. Radiolarians are poorly preserved due to highly recrystallization which makes them difficult to identify in detail; although thin-sections of the rock samples show high abundances of radiolarian tests. However, some characteristics of these faunas are present and can be determined as *Triassocampe* sp., *Eptingium* sp. and *Archaeocenosphaera* sp.. These radiolarians are common in the Middle Triassic time period so the section can be assigned to this age (Feng et al., 2002). The Den Chai locality is covered mainly by Triassic clastic rocks with some Pleistocene basalts (Geological Survey Division, 1999). The studied section was observed at 88 km of Highway 101 in the area of Den Chai District, Phrae Province. This section consists of chert and siliceous shale beds with claystone partings underlain by mudstones and shales while being unconformably overlain by basalts. Due to an intensely-folded sequence, total thickness is difficult to determine but thickness of the studied section is approximately 3 m. These cherts and siliceous shales are maroon in color with the bed between 1.5 and 8 cm thick. The radiolarians show that the age of this sequence is Middle Triassic (Thassanapak et al., 2007).

MATERIALS AND METHODS

Middle Triassic radiolarian cherts from Chiang Dao, Lamphun and Den Chai were subjected to geochemical analysis. It consisted of quantitative discrimination of major elements, trace elements and rare earth elements (REEs). For sample preparation, five samples from each section were crushed into small fragments and then selected by handpicking under a microscope to avoid contamination with Fe and Mn coatings and calcite veins. Selected sample fragments were pulverized in a vibratory cup mill. Concentrations of major elements were analyzed by X-ray fluorescence (XRF) spectrometry technique using Oxford ED2000 instrument at Suranaree University of Technology. REEs as well as trace elements were determined by inductively coupled plasma-mass spectrometry (ICP-MS) technique using Agilent 7500a at State Key Laboratory of Geological Processes and Mineral Resources, China University of Geosciences, Wuhan. Range of detection limit was 0.003 to 0.1 μg/g for heavier mass elements and 0.01 to 1 μg/g for lighter elements. Analytical precision is generally better than 5% for REEs and 6% for trace elements. REE abundances are normalized to North American Shale Composite (NASC) with normalized values as proposed by Gromet et al. (1984). Cerium anomalies (Ce/Ce*) were calculated from $Ce/Ce^*=Ce_n/(La_n \times Pr_n)^{1/2}$ and europium anomalies (Eu/Eu*) were derived from $Eu/Eu^*=Eu_n/(Sm_n \times Gd_n)^{1/2}$ (Taylor and McLennan, 1985). The ratio of HREE relative to LREE is presented as a NASC-normalized La_n/Yb_n ratio (Chen et al., 2006). Depositional setting of cherts is interpreted mainly by the La_n/Ce_n vs. $Al_2O_3/(Al_2O_3+Fe_2O_3)$ ratio (Murray, 1994). The origin of cherts is deduced from the Fe-Al-Mn diagram in which Fe and Mn components represent hydrothermal origin while Al indicates terrigenous input (Yamamoto, 1987; Adachi et al., 1986).

GEOCHEMISTRY

Major Elements

The silica content in cherts is relatively high and the content in Chiang Dao and Lamphun sections is higher than that from Den Chai (Table 1). It varies from (81.41–90.69) wt.% and (79.30–93.51) wt.% in Chiang Dao and Lamphun samples, respectively. It ranges between 68.48 wt.% and 77.50 wt.% in cherts from Den Chai. The lowest silica content in the three samples, from Den Chai, was observed with an increased phosphorus content ((3.63–5.68) wt.%). Correlation coefficient values (*r*) of silica with other major elements are generally highly negative (Table 2). Generally, the Si/(Si+Al+Fe) ratios from our samples are high and range between 0.92 and 0.99. The $Al_2O_3/(Al_2O_3+Fe_2O_3)$ ratios are intermediate in Den Chai (0.45) and high in Chiang Dao and Lamphun (0.78 and 0.74, respectively).

The aluminium content in all samples is relatively high and the highest content was observed in Den Chai cherts (4.58 wt.%). In Chiang Dao and Lamphun, the content varies from (1.11–3.63) wt.% and (0.69–2.40) wt.%, respectively. A highly positive correlation between aluminium and titanium, iron, manganese, magnesium, calcium and potassium (0.91–1.00) was determined for cherts from Chiang Dao. Samples from Den Chai exhibit a relatively high positive correlation between aluminium and titanium, iron, magnesium and phosphorus (0.86–0.97). In samples from Lamphun, aluminium shows a high positive correlation to titanium, magnesium, manganese and potassium (0.91–1.00).

The highest value of TiO_2 content was observed in Den Chai samples (0.08 wt.% to 0.17 wt.%). The titanium content in Chiang Dao and Lamphun was found to be between (0.02–0.08) wt.% and (0.01–0.07) wt.%, respectively. Correlation coefficient values of titanium from Chiang Dao samples are highly positive to most of the other elements (0.97–1.00). The situation in Lamphun is similar to that of Chiang Dao. However, Den Chai samples show a positive correlation of titanium to aluminum and iron.

The potassium content was the highest in cherts from Den Chai and varies from 1.07 wt.% to 2.15 wt.%. Lower content was found in Chiang Dao samples lying between 0.20 wt.% and 2.20 wt.%. The lowest content reported was from Lamphun (0.04 wt.% to 1.52 wt.%). With the exception of silica and sodium, potassium showed a highly positive correlation to most of the elements in Chiang Dao samples (0.92–1.00). For Lamphun samples, potassium exhibited a highly positive correlation to titanium, aluminium, magnesium, and calcium (0.93–1.00). However, in Den Chai, only sodium showed a relatively highly positive correlation to potassium (0.95).

The iron content was the highest in Den Chai samples (3.10 wt.% to 5.78 wt.%). It ranged between (0.16–1.42) wt.% and (0.22–0.51) wt.% in Chiang Dao and Lamphun, respectively. Iron showed a highly positive correlation to most of the elements (0.93–1.00) in samples from Chiang Dao. In Lamphun samples, iron has a slightly lower positive correlation to titanium (0.82), while a highly positive correlation of iron to aluminium titanium, manganese and potassium (0.86–0.98) is revealed from Den Chai samples.

Phosphorous content was observed in only three samples from Den Chai, which were between 3.63 wt.% and 5.68 wt.%. An increased phosphorous content was compatible with decreased silica content represented by a highly negative correlation coefficient between these elements. By contrast, phosphorous showed a moderately to highly positive correlation to aluminium, iron, and manganese (0.86–0.88).

Trace Elements

The majority of the cherts exhibit low trace element contents, less than 100 mg/kg (Table 3). However, most of W and Ba contents from Chiang Dao are high, exceeding 100 mg/kg. The highest contents of element are shown by Co from Lamphun and Ba from Den Chai. In order to reveal a relationship between trace and major elements, selected elements were subjected to correlation coefficient analysis (Table 2). As a result, moderately to highly positive (0.58–0.98) correlations between trace elements (Cr, Rb, Zr, Hf and Th) and major elements (TiO_2, Al_2O, MgO, and K_2O) were registered in samples from the Chiang Dao section. While the correlation coefficient values between Mo, Ni, and Zn and the aforementioned major elements are mostly low positive. By contrast, there were low correlations (-0.10–0.37) between these elements in the Lamphun samples. In Den Chai

Table 1 Major element concentrations as weight percentage (wt.%) and major element ratios

	SiO_2	TiO_2	Al_2O_3	Fe_2O_3	MnO	MgO	CaO	Na_2O	K_2O	P_2O_5	Si/(Si+Al+Fe)	Al/(Al+Fe)
Chiang Dao												
CD3	81.41	0.08	3.63	1.42	0.04	0.06	8.24	0.12	2.23		0.96	0.72
CD100	89.34	0.02	1.41	0.40	0.01	0.04	4.76	0.04	0.47		0.98	0.78
CD152	90.69	0.02	1.11	0.16	0.02	0.01	5.00	0.18	0.30		0.99	0.87
CD274	90.37	0.02	1.23	0.23	0.01		4.06	0.09	0.20		0.99	0.84
CD314	81.45	0.07	3.61	1.40	0.03	0.07	8.16		2.20		0.96	0.72
Geomean	86.54	0.03	1.91	0.49	0.02	0.04	5.79	0.09	0.67		0.97	0.78
Stdv	4.79	0.03	1.30	0.63	0.01	0.03	2.00	0.06	1.04		0.02	0.07
Lamphun												
LP1	92.16	0.02	0.95	0.45	0.03		2.75	0.05	0.08		0.99	0.68
LP8	93.51	0.01	0.69	0.24	0.03	0.02	2.65	0.07			0.99	0.74
LP29	91.32	0.01	0.70	0.31	0.08	0.01	3.14	0.41			0.99	0.69
LP33	92.52	0.01	0.78	0.22	0.03	0.02	2.89	0.01	0.04		0.99	0.78
LP37	79.30	0.07	2.40	0.51	0.04	0.08	8.96		1.52		0.97	0.82
Geomean	89.60	0.02	0.97	0.33	0.04	0.02	3.59	0.06	0.17		0.99	0.74
Stdv	5.90	0.03	0.73	0.13	0.02	0.03	2.74	0.19	0.84		0.01	0.06
Den Chai												
DC2	77.50	0.08	2.35	3.10	1.37	0.22	10.66	0.07	1.07		0.95	0.43
DC10	76.76	0.09	3.50	3.92	1.13	0.29	8.65	0.52	2.11		0.94	0.47
DC16	71.34	0.11	4.24	4.70	1.22	0.33	8.84	0.52	2.15	3.95	0.93	0.47
DC20	68.48	0.15	4.58	5.44	1.25	0.35	8.60	0.65	2.10	5.68	0.92	0.46
DC23	71.93	0.17	4.48	5.78	1.47	0.32	7.51	0.36	1.51	3.63	0.92	0.44
Geomean	73.12	0.12	3.72	4.48	1.28	0.30	8.80	0.34	1.73	4.33	0.93	0.45
Stdv	3.82	0.04	0.93	1.10	0.13	0.05	1.14	0.22	0.48	1.10	0.01	0.02

Geomean. geometric mean; Stdv. standard deviation; Si/(Si+Al+Fe). $SiO_2/(SiO_2+Al_2O_3+Fe_2O_3)$; Al/(Al+Fe). $Al_2O_3/(Al_2O_3+Fe_2O_3)$; Fe_2O_3. total iron content.

Section, Cr, Zr, Hf, Ni, Cu, and Zn showed moderately to highly positive correlations (0.79–0.99) to the major elements, while the others show low positive correlations.

Rare Earth Elements

REE contents from our samples were very low in comparison to NASC values (Table 4). The samples from Den Chai showed relatively higher REE content than those from Chiang Dao and Lamphun. Total REE content (ΣREE) from Den Chai ranged between 44.45 and 84.59 mg/kg, while ΣREE from Chiang Dao and Lamphun varied from 15.52 to 73.12 mg/kg and 5.11 to 25.58mg/kg, respectively.

The concentration of La was relatively high in Den Chai samples, between 7.87 and 15.85 mg/kg. The content of this element ranged from 0.89 to 5.47 mg/kg and 2.65 to 12.52 mg/kg in Lamphun and Chiang Dao, respectively. The Ce/Ce* ratios in most of the samples were slightly low (Geometric means; 0.85 to 0.93, also in brackets below). This situation is similar to that of Eu/Eu* ratios (0.91 to 0.94). The La_n/Ce_n ratios from all localities were slightly low (0.91 to 0.94). The comparison between LREE and HREE, represented by La_n/Yb_n ratios, was low in most of the samples (0.62 to 0.85). The relationship between LREE and HREE can also be deduced from the diagrams of NASC-normalized relative REE abundances (Fig. 2). As a result, REE distribution patterns from all sections were slightly flat and exhibited

Table 2 Correlation coefficient values of major elements and trace elements

Chiang Dao (*N*=5)																		
	SiO_2	TiO_2	Al_2O_3	CaO	MgO	K_2O	Fe_2O_3	Na_2O	MnO	Cr	Rb	Zr	Hf	Th	Mo	Ni	Cu	Zn
SiO_2	1.00																	
TiO_2	-1.00	1.00																
Al_2O_3	-1.00	1.00	1.00															
CaO	-0.98	0.99	0.98	1.00														
MgO	-0.92	0.89	0.91	0.89	1.00													
K_2O	-1.00	1.00	1.00	0.99	0.92	1.00												
Fe_2O_3	-1.00	0.99	1.00	0.98	0.93	1.00	1.00											
Na_2O	0.42	-0.36	-0.42	-0.29	-0.62	-0.38	-0.44	1.00										
MnO	-0.94	0.97	0.95	0.97	0.77	0.96	0.93	-0.16	1.00									
Cr	-0.62	0.58	0.61	0.56	0.79	0.60	0.62	-0.85	0.43	1.00								
Rb	-0.62	0.61	0.62	0.60	0.68	0.61	0.61	-0.54	0.54	0.93	1.00							
Zr	-0.63	0.62	0.63	0.59	0.62	0.62	0.62	-0.13	0.57	0.87	0.98	1.00						
Hf	-0.61	0.60	0.61	0.59	0.63	0.60	0.60	-0.09	0.56	0.89	0.99	0.99	1.00					
Th	-0.98	0.98	0.98	0.97	0.89	0.98	0.98	-0.60	0.95	0.68	0.74	0.75	0.74	1.00				
Mo	-0.16	0.16	0.18	0.02	-0.06	0.12	0.17	-0.61	0.14	-0.21	-0.21	-0.04	-0.15	0.11	1.00			
Ni	-0.55	0.51	0.54	0.50	0.71	0.54	0.56	0.25	0.38	0.99	0.94	0.90	0.92	0.63	-0.19	1.00		
Cu	-0.87	0.86	0.87	0.83	0.86	0.86	0.87	-0.28	0.78	0.88	0.92	0.92	0.91	0.93	0.03	0.87	1.00	
Zn	-0.61	0.60	0.61	0.60	0.67	0.61	0.60	-0.03	0.55	0.92	1.00	0.98	0.99	0.73	-0.24	0.93	0.91	1.00
Lamphun (*N*=5)																		
	SiO_2	TiO_2	Al_2O_3	CaO	MgO	K_2O	Fe_2O_3	Na_2O	MnO	Cr	Rb	Zr	Hf	Th	Mo	Ni	Cu	Zn
SiO_2	1.00																	
TiO_2	-0.97	1.00																
Al_2O_3	-0.98	1.00	1.00															
CaO	-1.00	0.97	0.98	1.00														
MgO	-0.90	0.88	0.91	0.94	1.00													

Continued

Lamphun (N=5)																		
	SiO_2	TiO_2	Al_2O_3	CaO	MgO	K_2O	Fe_2O_3	Na_2O	MnO	Cr	Rb	Zr	Hf	Th	Mo	Ni	Cu	Zn
K_2O	-0.99	0.98	1.00	1.00	0.93	1.00												
Fe_2O_3	-0.74	0.82	0.78	0.71	0.45	0.73	1.00											
Na_2O	0.26	-0.46	-0.42	-0.30	-0.45	-0.38	-0.22	1.00										
MnO	-0.06	-0.16	-0.11	0.01	-0.19	-0.08	0.02	0.94	1.00									
Cr	0.21	-0.45	-0.38	-0.25	-0.32	-0.33	-0.39	0.90	0.90	1.00								
Rb	-0.20	0.15	0.17	0.25	0.37	0.23	-0.06	0.25	0.07	-0.03	1.00							
Zr	0.61	-0.46	-0.51	-0.58	-0.46	-0.53	-0.30	-0.46	-0.47	-0.43	0.36	1.00						
Hf	0.41	-0.30	-0.34	-0.37	-0.20	-0.33	-0.28	-0.34	-0.45	-0.42	0.63	0.94	1.00					
Th	0.31	-0.17	-0.21	-0.26	-0.10	-0.21	-0.18	-0.42	-0.54	-0.54	0.62	0.92	0.99	1.00				
Mo	0.36	-0.51	-0.49	-0.41	-0.59	-0.47	-0.16	0.98	0.89	0.84	-0.01	-0.10	-0.18	-0.30	1.00			
Ni	0.61	-0.44	-0.52	-0.61	-0.62	-0.56	-0.08	-0.34	-0.33	-0.38	0.13	0.92	0.78	0.76	0.09	1.00		
Cu	0.75	-0.61	-0.65	-0.74	-0.63	-0.69	-0.49	-0.92	-0.54	-0.26	-0.60	0.44	0.19	0.17	-0.21	0.45	1.00	
Zn	0.54	-0.34	-0.42	-0.53	-0.52	-0.47	-0.03	-0.51	-0.49	-0.55	0.09	0.92	0.78	0.79	-0.10	0.98	0.50	1.00

Den Chai (N=5)																			
	SiO_2	TiO_2	Al_2O_3	CaO	MgO	K_2O	Fe_2O_3	Na_2O	MnO	P_2O_5	Cr	Rb	Zr	Hf	Th	Mo	Ni	Cu	Zn
SiO_2	1.00																		
TiO_2	-0.78	1.00																	
Al_2O_3	-0.89	0.86	1.00																
CaO	0.57	-0.85	-0.87	1.00															
MgO	-0.91	0.75	0.97	-0.77	1.00														
K_2O	-0.51	0.20	0.65	-0.49	0.77	1.00													
Fe_2O_3	-0.86	0.98	0.95	-0.88	0.87	0.39	1.00												
Na_2O	-0.69	0.44	0.79	-0.62	0.90	0.95	0.60	1.00											
MnO	-0.05	0.43	-0.03	-0.08	-0.22	-0.78	0.26	-0.61	1.00										
P_2O_5	-1.00	0.78	0.87	-0.55	0.88	0.45	0.86	0.63	0.12	1.00									

Continued

Den Chai (*N*=5)																		
	SiO_2	TiO_2	Al_2O_3	CaO	MgO	K_2O	Fe_2O_3	Na_2O	MnO	P_2O_5	Cr	Rb	Zr	Hf	Th	Mo	Ni	Cu	Zn
Cr	-0.75	0.98	0.77	-0.75	0.66	0.08	0.93	-0.24	0.51	0.15	1.00								
Rb	-0.45	0.15	0.59	-0.49	0.73	1.00	0.33	0.28	-0.82	0.63	0.03	1.00							
Zr	-0.80	0.87	0.82	0.49	0.80	0.39	0.87	-0.34	0.12	0.65	0.90	0.37	1.00						
Hf	-0.80	0.87	0.80	0.20	0.79	0.36	0.86	-0.36	0.14	0.66	0.90	0.35	1.00	1.00					
Th	-0.77	0.70	0.66	0.16	0.70	0.33	0.71	-0.46	0.05	0.85	0.78	0.33	0.94	0.95	1.00				
Mo	-0.74	0.51	0.52	0.31	0.62	0.33	0.54	-0.45	-0.07	0.96	0.60	0.34	0.82	0.84	0.96	1.00			
Ni	-0.95	0.91	0.96	0.76	0.91	0.46	0.97	0.30	0.18	0.51	0.85	0.40	0.82	0.81	0.70	0.58	1.00		
Cu	-0.99	0.86	0.92	0.62	0.91	0.46	0.92	0.22	0.15	0.93	0.82	0.40	0.83	0.83	0.76	0.69	0.98	1.00	
Zn	-0.89	0.82	0.99	0.73	0.99	0.71	0.92	0.26	-0.12	0.92	0.74	0.66	0.83	0.81	0.69	0.57	0.94	0.91	1.00

Table 3 Trace element concentrations (mg/kg)

	Sc	V	Cr	Co	Ni	Cu	Zn	Ga	Rb	Sr	Y	Zr	Nb	Mo	Cs	Ba	Hf	Ta	W	Tl	Pb	Th	U
Chiang Dao																							
CD3	4.02	7.18	7.35	62.55	1.24	1.42	1.64	1.98	11.42	13.46	5.68	14.77	2.70	1.56	0.58	120.39	0.29	0.56	153.63	0.09	1.67	2.67	0.94
CD100	3.43	10.63	10.08	99.18	2.05	0.92	1.83	2.68	13.54	13.79	3.66	10.63	1.20	0.60	0.48	96.08	0.28	0.34	180.01	0.06	1.19	0.94	0.40
CD152	2.98	5.65	5.00	55.00	0.87	0.65	1.69	2.14	10.53	29.46	5.55	10.53	1.21	0.30	0.49	90.23	0.28	0.34	180.01	0.06	1.19	0.94	0.40
CD274	3.46	6.12	5.92	103.76	1.22	0.82	1.39	1.94	9.28	14.87	3.69	17.50	1.16	2.04	0.48	81.81	0.30	0.52	87.95	0.07	1.37	0.91	0.53
CD314	7.51	21.43	15.60	17.57	3.58	2.38	5.10	9.16	48.40	37.40	14.40	67.83	3.23	0.87	1.32	227.29	1.70	0.35	19.09	0.28	3.01	3.18	0.63
Geomean	4.03	8.92	8.07	57.38	1.58	1.11	2.05	2.89	14.89	19.80	5.72	18.14	1.71	0.87	0.61	114.18	0.41	0.41	96.47	0.09	1.58	1.47	0.55
Stdv	1.85	6.57	4.26	35.33	1.09	0.70	1.56	3.13	16.71	11.00	4.47	24.53	0.99	0.71	0.37	59.96	0.63	0.11	69.75	0.09	0.77	1.11	0.22
Lamphun																							
LP1	0.96	3.80	4.36	157.45	5.45	5.60	6.81	1.20	3.95	5.27	4.11	7.88	0.40	0.50	0.24	18.54	0.17	0.43	86.52	0.02	3.85	0.47	0.27
LP8	1.64	5.79	5.42	167.16	5.22	4.35	6.30	1.78	8.08	12.17	2.96	9.32	0.65	0.39	0.46	38.23	0.25	0.47	103.45	0.03	5.26	0.74	0.28
LP29	0.89	2.79	12.67	106.69	3.63	2.69	2.87	1.01	5.80	2.08	1.42	5.72	0.36	0.96	0.33	19.97	0.13	0.37	59.37	0.05	1.50	0.27	0.19
LP33	0.74	1.70	7.36	186.47	3.24	6.27	3.11	0.91	3.59	3.39	4.15	5.89	0.15	0.31	0.23	13.46	0.13	0.22	34.81	0.03	2.14	0.30	0.20
LP37	1.01	2.67	5.14	149.52	2.89	1.58	2.55	1.08	6.45	3.21	2.03	5.12	0.32	0.25	0.37	22.30	0.13	0.41	44.62	0.05	1.88	0.36	0.18
Geomean	1.01	3.08	6.47	150.92	3.96	3.65	3.96	1.16	5.33	4.29	2.71	6.62	0.34	0.43	0.31	21.17	0.16	0.37	60.72	0.03	2.62	0.40	0.22
Stdv	0.35	1.55	3.36	29.57	1.17	1.96	2.05	0.35	1.85	4.05	1.22	1.76	0.18	0.28	0.10	9.37	0.05	0.10	28.71	0.01	1.58	0.19	0.05
Den Chai																							
DC2	4.30	18.56	9.44	73.73	5.20	8.65	45.46	5.95	26.65	30.66	8.15	38.26	2.70	0.19	2.06	115.39	1.09	0.64	39.19	0.18	6.54	2.30	1.02
DC10	5.41	22.03	9.88	54.70	6.50	10.26	61.71	8.67	49.17	37.88	12.38	57.07	3.60	0.21	4.40	190.80	1.55	0.58	24.78	0.29	7.23	2.99	1.24
DC16	6.59	26.74	10.86	26.68	9.61	18.88	69.49	8.53	47.70	57.25	10.85	51.49	2.75	0.20	4.26	190.12	1.41	0.35	10.59	0.28	8.08	2.57	1.24
DC20	8.29	32.37	15.19	21.40	10.79	23.38	75.20	9.56	47.99	69.85	19.37	92.82	4.93	2.64	4.27	191.63	2.58	0.53	5.61	0.27	11.20	6.70	1.53
DC23	8.03	38.91	16.52	37.57	10.60	19.99	71.03	8.68	34.45	100.91	16.46	79.43	4.09	0.55	4.35	148.58	2.18	0.53	9.99	0.21	15.14	4.23	0.81
Geomean	6.34	26.78	12.05	38.67	8.20	15.09	63.61	8.17	40.07	54.22	12.84	60.77	3.52	0.41	3.73	164.15	1.68	0.52	14.20	0.24	9.17	3.47	1.14
Stdv	1.70	8.12	3.25	21.47	2.54	6.43	11.75	1.37	10.12	27.95	4.47	22.00	0.94	1.06	1.01	34.31	0.60	0.11	13.85	0.05	3.56	1.80	0.27
—	—	—	—	—	—	—	—	—	—	—	—	—	—	—	—	—	—	—	—	—	—	—	—

Geomean. geometric mean; Stdv. standard deviation.

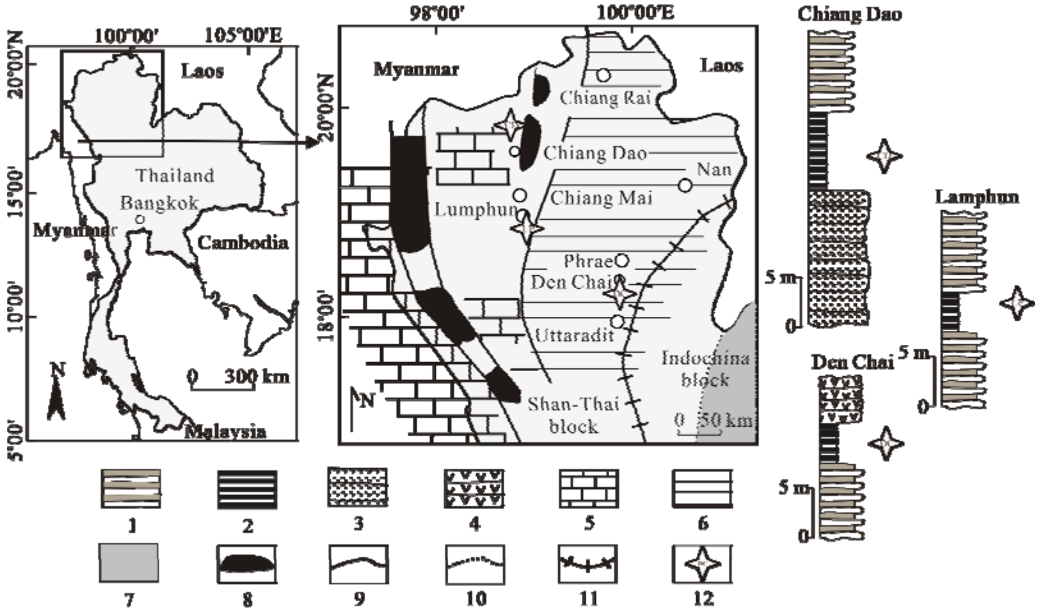

Figure 1. Triassic paleogeographic map (based on Chonglakmani, 1999) showing the studied sections. The studied sections comprise Chiang Dao (CD), Lamphun (LP) and Den Chai (DC). 1. Mudstones/shales; 2. cherts and siliceous shales; 3. sandstones; 4. Pleistocene basalts; 5. continental platform facies; 6. the marine associated with volcanic facies; 7. continental facies; 8. deep marine facies; 9. boundary; 10. inferred boundary; 11. Nan-Uttaradit suture; 12. study section.

LREE depletion with HREE enrichment. The Ce anomalies were obviously low in Lamphun and Den Chai, while Eu anomalies were not significant in the majority of the samples.

DISCUSSION ON THE ORIGIN AND DEPOSITIONAL ENVIRONMENT OF CHERTS

Geochemistry of radiolarian cherts is an important tool to elucidate their depositional environment and paleogeography of particular areas or regions. However, some of the major elements, including Si, Ca, Mn, Mg and P are inappropriate to use because of their diagenetic fractionation and migration characteristics (Halamić et al., 2001). In our study, some of geochemical contents and ratios were analyzed in order to discriminate the origin of cherts and their depositional environment. For the origin of cherts, the majority of our samples were located in the field of non-hydrothermal as shown in the Fe-Al-Mn diagram which was developed by Adachi et al. (1986) and Yamamoto (1987) (Fig. 3). In addition, the high ratios of Si/(Si+Al+Fe) (range between 0.92 and 0.99) are compatible with biogenic origin as proposed by Rangin et al. (1981). However, highly negative correlations between SiO_2 and the majority of the other major elements can be explained by dilution process. In the depositional environment, Al, Ti, Fe and REEs are generally unaffected by diagenetic alteration so these elements can be largely used for depositional environment implication (Murray et al., 1990). It can be suggested that high content of Al, Ti and K is a good indicator for clastic or detrital components (terrigenous input), while high Fe content is a good representative of hydrothermal influence. The Chiang Dao and Lamphun sections showed relatively high Al content compared to Fe, which implies that the depositional environment was closer to the continent than the hydrothermal vent system. In contrast, Den Chai samples exhibited high Fe content in comparison to Al which could indicate hydrothermal influences during deposition of the sediments. However, this interpretation is improbable since high Ce anomalies (from 0.81 to 0.91) giving indications of high detrital inputs were registered on samples from this section. A good correlation between Fe, Al and Ti supports that part of Fe was a terrigenous input. In addition, the Ce anomalies from all studied sections ranged between 0.74 and 1.05 and all of them were consistent with those of the continental margin (0.67–1.52) from Murray et al. (1990).

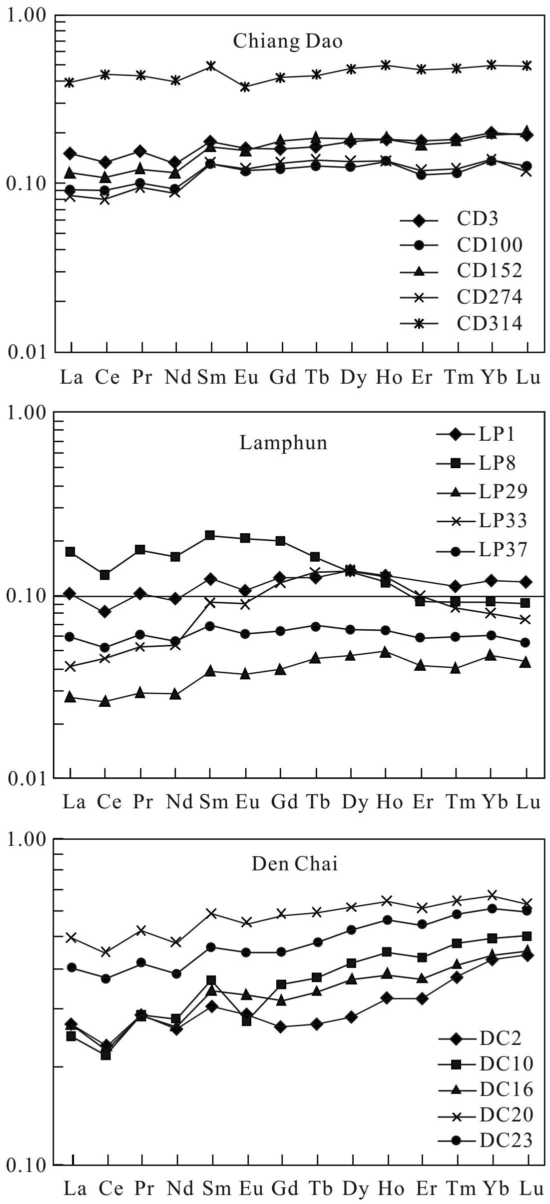

Figure 2. NASC normalized REE distribution diagrams of chert samples.

For the trace elements, contents of Ba, Sr, V and Co can be altered by diagenetic processes; thus, these data should be considered with caution (Murrey, 1994). The contents of Cr, Zr, Hf , Rb, Th and part of V are more applicable for depositional environments in which high contents indicate high input of detrital and clastic materials (Halamić et al., 2001). However, Cr content can be enriched by hydrothermal influence, and this element is partly mobile (Kametaka et al., 2005; Marchig et al., 1982). Our samples showed moderate to high contents of the aforementioned elements, which is in agreement with the continental margin origin. Additionally, the majority of these elements show a good correlation with Al and Ti, except for the samples from Lamphun. For the Lamphun case, it indicates that at least part of these trace elements were derived from a difference source. While Cr, Zr, Hf , Rb and Th in Lamphun were mostly in good mutual correlation with an exceptional of Cr which is probably explained by its partly mobile characteristic.

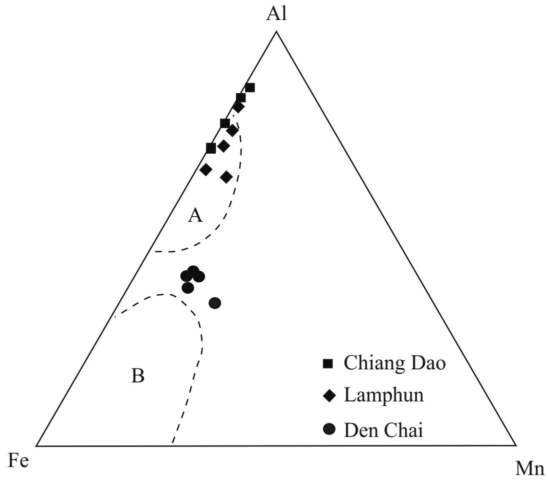

Figure 3. Al-Fe-Mn diagram. Fields of non-hydrothermal (A) and hydrothermal (B) are from Adachi et al. (1986).

The NASC-normalized REE abundance patterns are relatively flat with slight enrichment of HREE in comparison with LREE (La_n/Yb_n; geometric means 0.62 to 0.85, also in brackets below) (Fig. 2, Table 4). These patterns reveal relatively high terrigenous inputs which are closely related to the continental margin. This interpretation corresponds with the low values of Eu anomalies which are exhibited in all sections (Eu/Eu*, 0.91–0.94). Generally, sediments related to vent fluids are characterized by highly positive Eu anomalies (German et al., 1990). While negative Ce anomalies caused by depletion of Ce concentration through the water column indicate the typical characters of marine basins (Murray et al., 1990). Slightly low Ce anomalies (0.85–0.93) from our studied samples reveal some connection to marine basins. However, these anomalies are not as significantly low as observed in open-ocean basins (0.5–0.76 from Murray et al., 1991) so our studied sections have more connection with the continental margin than the open-ocean basins.

Table 4 Rare earth element concentrations (mg/kg)

	La	Ce	Pr	Nd	Sm	Eu	Gd	Tb	Dy	Ho	Er	Tm	Yb	Lu	ΣREE	Ce/Ce*	Eu/Eu*	La_n/Yb_n	La_n/Ce_n
NASC	32	73	7.9	33	5.7	1.24	5.2	0.85	5.2	1.04	3.4	0.5	3.1	0.48	172.61				
Chiang Dao																			
CD3	4.71	9.51	1.20	4.28	0.99	0.20	0.82	0.14	0.91	0.19	0.60	0.09	0.61	0.09	24.33	0.87	0.96	0.75	1.13
CD100	2.91	6.55	0.79	3.02	0.73	0.14	0.62	0.11	0.65	0.14	0.38	0.06	0.42	0.06	16.57	0.94	0.94	0.68	1.01
CD152	3.67	7.84	0.95	3.77	0.92	0.19	0.93	0.16	0.94	0.19	0.57	0.09	0.60	0.10	20.91	0.91	0.91	0.59	1.07
CD274	2.65	5.80	0.74	2.87	0.74	0.15	0.69	0.12	0.69	0.14	0.40	0.06	0.42	0.06	15.52	0.90	0.92	0.61	1.04
CD314	12.52	31.54	3.44	13.29	2.74	0.46	2.18	0.37	2.45	0.52	1.59	0.24	1.54	0.23	73.12	1.05	0.83	0.79	0.91
Geomean	4.41	9.78	1.18	4.50	1.06	0.21	0.93	0.16	0.99	0.20	0.61	0.09	0.63	0.09	24.90	0.93	0.91	0.68	1.03
Stdv	4.12	10.88	1.14	4.42	0.86	0.13	0.65	0.11	0.75	0.16	0.50	0.08	0.47	0.07	24.31	0.07	0.05	0.08	0.08
Lamphun																			
LP1	3.25	5.86	0.80	3.13	0.70	0.13	0.64	0.11	0.70	0.13	0.40	0.05	0.38	0.06	16.33	0.79	0.86	0.83	1.26
LP8	5.47	9.33	1.39	5.28	1.20	0.25	1.02	0.14	0.70	0.12	0.31	0.05	0.28	0.04	25.58	0.74	0.99	1.86	1.34
LP29	0.89	1.92	0.23	0.95	0.22	0.05	0.21	0.04	0.24	0.05	0.14	0.02	0.15	0.02	5.11	0.92	0.96	0.58	1.05
LP33	1.30	3.29	0.41	1.75	0.52	0.11	0.60	0.11	0.72	0.13	0.34	0.04	0.25	0.04	9.59	0.98	0.87	0.51	0.90
LP37	1.86	3.75	0.48	1.84	0.39	0.08	0.33	0.06	0.34	0.07	0.20	0.03	0.19	0.03	9.64	0.86	0.91	0.96	1.13
Geomean	2.07	4.19	0.55	2.19	0.52	0.10	0.48	0.08	0.49	0.09	0.26	0.04	0.24	0.03	11.46	0.85	0.92	0.85	1.13
Stdv	1.86	2.89	0.46	1.70	0.38	0.08	0.32	0.04	0.23	0.04	0.11	0.01	0.09	0.01	7.97	0.10	0.06	0.54	0.17
Den Chai																			
DC2	8.56	16.77	2.27	8.57	1.74	0.36	1.36	0.23	1.46	0.34	1.09	0.19	1.31	0.21	44.45	0.83	1.02	0.64	1.17
DC10	7.87	15.63	2.26	9.20	2.08	0.34	1.84	0.32	2.15	0.46	1.46	0.24	1.53	0.24	45.62	0.81	0.76	0.50	1.15
DC16	8.53	16.75	2.24	8.70	1.95	0.41	1.65	0.29	1.92	0.40	1.26	0.21	1.36	0.22	45.89	0.83	1.00	0.61	1.16
DC20	15.85	32.61	4.09	15.84	3.34	0.68	3.04	0.50	3.19	0.67	2.07	0.32	2.07	0.30	84.59	0.88	0.94	0.74	1.11
DC23	12.84	26.98	3.27	12.70	2.62	0.56	2.33	0.41	2.71	0.58	1.84	0.29	1.89	0.29	69.29	0.91	0.99	0.66	1.09
Geomean	10.32	20.77	2.74	10.66	2.28	0.45	1.97	0.34	2.21	0.48	1.50	0.24	1.60	0.25	55.89	0.85	0.94	0.62	1.13
Stdv	3.48	7.62	0.83	3.19	0.65	0.15	0.66	0.11	0.67	0.13	0.40	0.06	0.33	0.04	18.15	0.04	0.11	0.09	0.03

NASC. North American shale composite; Geomean. geometric mean; Stdv. standard deviation; $Ce/Ce^*=Ce_n/(La_n \times Pr_n)^{1/2}$; $Eu/Eu^*=Eu_n/(Sm_n \times Gd_n)^{1/2}$.

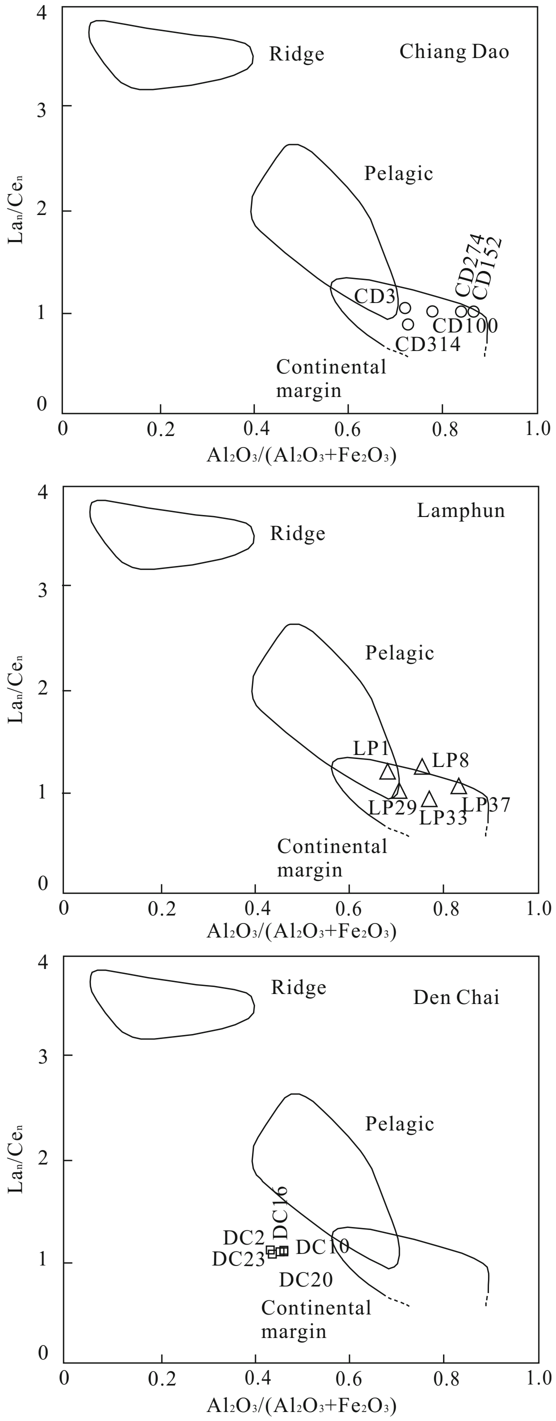

Figure 4. La_n/Ce_n vs. $Al_2O_3/(Al_2O_3+Fe_2O_3)$ discrimination diagrams. Fields of all settings are from Murray (1994).

The La_n/Ce_n vs. $Al_2O_3/(Al_2O_3+Fe_2O_3)$ discrimination diagrams show that the majority of cherts from our samples were deposited in the continental margin (residual basin, *s. str.*). However, the samples from Den Chai which were distributed outside all fields in the diagram are more closely related to the continental margin than the others (Fig. 4). This condition can be explained by the increased Fe content and low value of La_n/Ce_n ratio. The relatively high Fe content is a result of the addition of Fe derived from the continent during deposition, which can be explained by a good mutual correlation between Fe, Al and Ti as mentioned earlier (e.g., Halamić et al., 2001). This interpretation is compatible with geological evidence (e.g., Geological Survey Division, 1999; Charoenprawat et al., 1994; Hess and Koch, 1979) which indicates a close stratigraphic position between radiolarian cherts and the clastic sequences in all studied sections. However, some parts of these clastic sequences in Chiang Dao and Lamphun localities formerly assigned to Carboniferous and Permian should be changed to Middle Triassic as a consequence of Middle Triassic radiolarian occurrences (Thassanapak et al., 2011; Feng et al., 2002). Geological and geochemical data suggest that during Middle Triassic, radiolarian cherts were deposited within deeper part of the residual basin in which an accommodation space was possibly controlled by faults (Fig. 5). These data support a Late Variscan (Permian) extension of the continental margin as motioned by Helmcke (1985). The main Paleotethys which were subjected to closures during the Late Triassic should be located further to the west of these study localities. This scenario is in concordance with a current view of the Paleotethys in this region (e.g., Ferrari et al., 2008; Ueno, 2003; Chonglakmani, 2002; Wang et al., 2001; Helmcke, 1994).

CONCLUSION

The majority of Middle Triassic radiolarian cherts from the studied sections in Chiang Dao, Lamphun and Den Chai exhibit slightly high SiO_2 and they are mainly of biogenic origin. This origin is elucidated from the Si/(Si+Al+Fe) ratio and the Fe-Al-Mn diagram, which is compatible with low Eu anomalies. The silica content from these localities was possibly modified by diagenetic dissolution and migration processes as a result of a highly negative correlation between SiO_2 and most of the major elements. The La_n/Ce_n vs. $Al_2O_3/(Al_2O_3+Fe_2O_3)$ diagrams suggest that radiolarian cherts from all sections were deposited within the continental margin which can be correlated to a deeper part of the fault-controlled residual basin.

However, the samples from Den Chai were distributed outside all fields of the diagram because of relatively high Fe content and low La_n/Ce_n ratios. In this case, Fe content is partly derived from the continent which is suggested by a highly positive correlation with Al and Ti. Moreover, high Ce anomalies from all sections support the continental-margin environment of cherts. Slight enrichment of HREE compared to LREE from REE distribution diagrams (La_n/Yb_n (geometric mean 0.62 to 0.85)) indicates relatively high terrigenous input. Moderate to high contents of Cr, Zr, Hf , Rb and Th are also consistent with this interpretation.

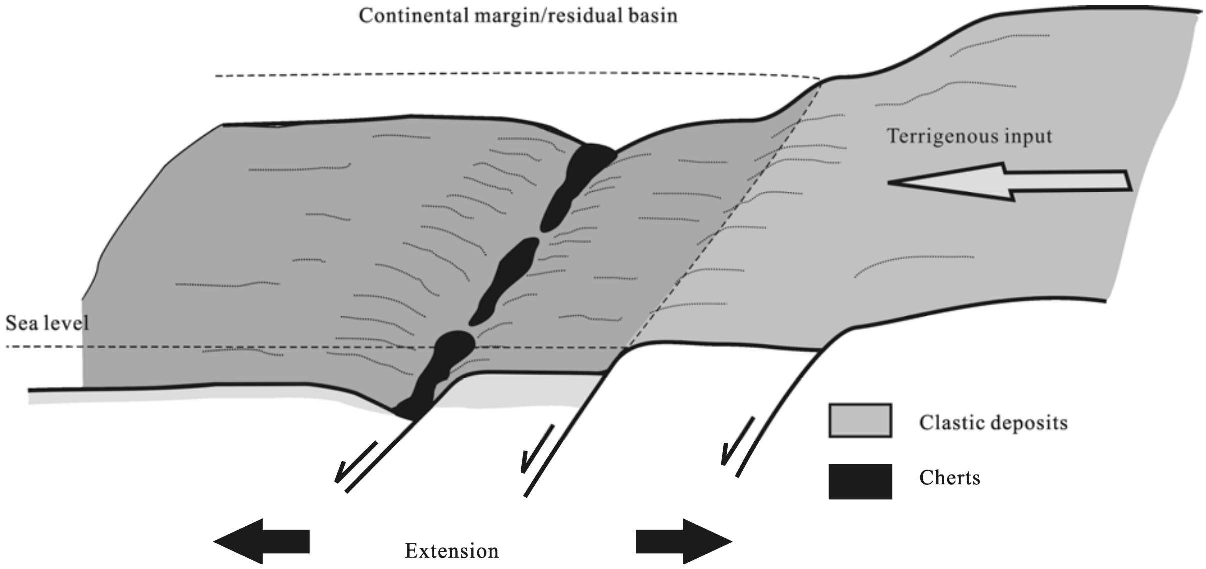

Figure 5. Depositional setting of Middle Triassic cherts from central part of northern Thailand.

ACKNOWLEDGMENTS

This study was completed with the financial support mainly provided by the NSFC (No. 40772143) and from the special fund of the State Key Laboratory of Geological Processes and Mineral Resources, China University of Geosciences. Financial support was also partly contributed by the Faculty of Science, Mahasarakham University. The study was conducted in Thailand and completed at China University of Geosciences (Wuhan). Many thanks are conveyed to the officials at the State Key Laboratory of Geological Processes and Mineral Resources, China University of Geosciences, Wuhan. We thank Wencheng Yang, Mei Ye and other Chinese colleagues from CUG for their help during the visit by Thai geologists. We appreciate the meaningful comments from Dr. J Halamić of Institute of Geology, Croatia, which have improved this manuscript. We are also indebted to Dr. J Dodgson of Mahasarakham University for English revision of the manuscript.

REFERENCES CITED

Adachi, M., Yamamoto, K., Sugisaki, R., 1986. Hydrothermal Chert and Associated Chert from the Northern Pacific, Their Geological Significance as Indication of Ocean Ridge Activity. *Sedimentary Geology*, 47: 125–148, doi:10.1016/0037-0738(86)90075-8

Caridroit, M., 1993. Permian Radiolarian from NW Thailand. In: Thanasuthipitak, T., ed., Proceeding of International Symposium on Biostratigraphy of Mainland Southeast Asia: Facies and Paleontology. Chiang Mai University, Thialand. 83–96

Chaodumrong, P., Burret, C., 1997. Early Late Triassic Continental Colliding between Shan-Thai and Indochina Terranes as Indicated by Occurrence of Fan Delta Red Beds of Pha Daeng Formation, Central North Thailand. In: Dheeradirok, P., Hinthong, C., Chaodumrong, P., et al., eds., Proceedings of International Conference on Stratigraphy and Tectonic Evolution of Southeast Asia and the South Pacific. Geological Survey Division, Department of Mineral Resources, Bangkok, Thailand. 143–157

Charoenprawat, A., Chuaviroj, S., Hinthong, C., et al., 1994. Geologic Map of Changwat Lampang, Scale 1 : 250 000. Department of Mineral Resources, Bangkok, Thailand

Chen, D. Z., Qing, H. R., Yan, X., et al., 2006. Hydrothermal Venting and Basin Evolution (Devonian, South China):

Constraints from Rare Earth Element Geochemistry of Chert. *Sedimentary Geology*, 183(3–4): 203–216

Chonglakmani, C., 1999. The Triassic System of Thailand: Implications for the Paleogeography of Southeast Asia. In: Rattanasatein, B., ed., Proceeding of International Symposium on Shallow Tethys (ST) 5. Department of Geological Sciences, Chiang Mai University. 486–495

Chonglakmani, C., 2002. Current Status of Triassic Stratigraphy of Thailand and Its Implication for Geotectonic Evolution. Proc. Symp. Geology of Thailand, Department of Mineral Resources, Bangkok, Thailand. 1–3

Chonglakmani, C., Grant-Mackie, J. A., 1993. Biostratigraphy and Facies Variation of the Marine Triassic Sequences in Thailand. In: Thanasuthipitak, T., ed., Proceeding of the International Symposium on Biostratigraphy of Mainland Southeast Asia: Facies and Paleontology. Chiang Mai University, Thailand. 97–123

Feng, Q. L., Chonglakmani, C., Helmcke, D., et al., 2002. Middle Triassic Radiolarian Fauna from Lumphun, Northern Thailand. In: Proceeding of the International Symposium on Geology of Thailand. Bangkok, Thailand. 26–31

Feng, Q. L., Chonglakmani, C., Helmcke, D., et al., 2005a. Correlation of Triassic Stratigrasphy between the Simao and Lampang-Phrae Basins: Implication for the Tectonopaleography of Southeast Asia. *Journal of Asian Earth Sciences*, 24: 777–785

Feng, Q. L., Malila, K., Wonganan, N., et al., 2005b. Permian and Triassic Radiolaria from Northwest Thailand: Palaeogeographical Implications. *Revue de Micropaleontologie*, 48(4): 237–255

Ferrari, O. M., Hochard, C., Stampfli, G. M., 2008. An Alternative Plate Tectonic Model for the Palaeozoic–Early Mesozoic Palaeotethyan Evolution of Southeast Asia (Northern Thailand-Burma). *Tectonophysics*, 451: 346–365

Geological Survey Division, 1999. Geological Map of Thailand, Scale 1 : 2 500 000. Department of Mineral Resources, Bangkok, Thailand

German, C. R., Klinkhammer, G. P., Edmond, J. M., et al., 1990. Hydrothermal Scavenging of Rare-Earth Elements in the Ocean. *Nature*, 345: 516–518

Gromet, L. P., Dymek, R. F., Haskin, L. A., et al., 1984. The "North American Shale Composite": Its Compilation, Major and Trace Element Characteristics. *Geochim. Cosmochim. Acta*, 48(12): 2469–2482, doi:10.1016/0016-7037(84)90298-9

Halamić, J., Marchig, V., Goričan, S., 2001. Geochemistry of Triassic Radiolarian Cherts in North-Western Croatia. *Geologica Carpathica*, 52(6): 327–342

Helmcke, D., 1985. The Permo–Triassic Paleotethys in Mainland Southeast-Asia and Adjacent Parts of China. *Geologische Rundschau*, 74(2): 215–228, doi:10.1007/BF01824893

Helmcke, D., 1994. Distribution of Permian and Triassic Syn-Orogenic Sediments in Central Mainland SE-Asia. In: Angsuwathana, P., Wongwanich, T., Tansathien, W., et al., eds., Proceeding of the International Symposium on Stratigraphic Correlation of Southeast Asia. Bangkok, Thailand. 123–128

Hess, A., Koch, K. E., 1979. Geologic Map of Northern Thailand, Scale 1 : 250 000, Sheet 4 (Chiang Dao). Federal Institute for Geosciences and Natural Resources, Germany

Jaeger, H., Stein, V., Wolfart, R., 1969. Fauna (Graptolithen Brachiopoden) der Unterdevonischen Schwarzschiefer Nord-Thailands. *Neues Jahrbuch für Geologie und Paläontologie. Abhandlungen*, 133: 171–190

Kamata, Y., Sashida, K., Ueno, K., et al., 2002. Triassic Radiolarian Faunas from the Mae Sariang Area, Northern Thailand and Their Paleogeographic Significance. *Journal of Asian Earth Sciences*, 20: 491–506, doi:10.1016/S1367-9120(01)00047-5

Kametaka, M., Takebe, M., Nagai, H., et al., 2005. Sedimentary Environments of the Middle Permian Phosphorite-Chert Complex from the Northeastern Yangtze Platform, China, the Gufeng Formation: A Continental Shelf Radiolarian Chert. *Sedimentary Geology*, 174(3/4): 197–222

Marchig, V., Gundlach H., Möller P., et al., 1982. Some Geochemical Indicators for Discrimination between Diagenetic and Hydrothermal Metalliferous Sediments. *Marine Geology*, 50(3): 241–256

Meesook, A., Suteethon, V., Chaodumrong, P., et al., 2002. Mesozoic Rocks of Thailand: A Summary. In: Montajit, N., Potisat, S., Wongwanich, T., et al., eds., Proceedings of the Symposium on Geology of Thailand. Department of Mineral Resources, Bangkok, Thailand. 82–94

Murray, R. W., 1994. Chemical Criteria to Identify the Depositional Environment of Chert: General Principles and Applications. *Sedimentary Geology*, 90: 213–232

Murray, R. W., Buchholtz ten Brink, M. R., Gerlach, D. C., et al., 1990. Rare Earth Elements as Indicators of Different Marine Depositional Environments in Chert and Shale. *Geology*, 18(3): 268–271

Murray, R. W., Buchholtz ten Brink, M. R., Gerlach, D. C., et al., 1991. Rare Earth, Major, and Trace Elements in Chert from the Franciscan Complex and Monterey Group, Californian: Assessing REE Sources to Fine-Grained Marine Sediments. *Geochim. Cosmochim. Acta*, 55(7): 1875–1895

Rangin, C., Steinberg, M., Bonnot-Courtois, C., 1981. Geochemistry of the Mesozoic Bedded Chert of Central Baja California (Vizcaino-Cedros-San Benito): Implication for Palaogeographic Reconstruction of an Old Oceanic Basin. *Earth and Planetary Science Letter*, 54: 313–322

Sashida, K., Igo, H., Hisada, K., et al., 1993. Occurrence of Paleozoic and Early Mesozoic Radiolarian in Thailand (Preliminary Report). *Journal of Southeast Asian Earth Sciences*, 8: 97–108

Taylor, S. R., McLennan, S. M., 1985. The Continental Crustal: Its Composition and Evolution. Blackwell, Oxford

Thassanapak, H., Chonglakmani, C., Feng, Q. L., et al., 2007. Middle Triassic Radiolarians from Den Chai Area, Northern Thailand. In: Tantiwanit, W., Raksasakulwong, L., Suteethorn, V., et al., eds., Proceeding of the International Conference on Geology of Thailand: Towards Sustainable Development and Sufficiency Economy. Bankkok, Thailand. 180–186

Thassanapak, H., Feng, Q. L., Grant-Mackie, J., et al., 2011. Middle Triassic radiolarian faunas from Chiang Dao, Northern Thailand. *Palaeoworld*, 20(2–3): 179–202, doi:10.1016/j.palwor.2010.11.001

Ueno, K., 2003. The Permian Fusulinoidean Faunas of the Sibumasu and Baoshan Blocks: Their Implication for the Paleogeographic and Paleoclimatologic Reconstruction of the Cimmerian Continent. *Palaeogeography*, *Palaeoclimatology*, *Paleoecology*, 193(1): 1–24

Wang, X. D., Ueno, K., Mizuno, Y., et al., 2001. Late Paleozoic Faunal, Climatic, and Geographic Changes in the Baochan Block as a Gondwana-Derived Continental Fragment in Southwest China. *Palaeogeography*, *Palaeoclimatology*, *Palaeoecology*, 170: 197–218

Yamamoto, K., 1987. Geochemical Characteristics and Depositional Environments of Cherts in the Franciscan and Shimanto Terranes. *Sedimentary Geology*, 52(1–2): 65–108